J|A|C|S
ARTICLES
Published on Web 02/15/2003

# Solvent-Induced Polymorphism of Three-Dimensional Hydrogen-Bonded Networks of Hexakis(4-carbamoylphenyl)benzene

Kenji Kobayashi,*,† Azumi Sato,‡ Shigeru Sakamoto,§ and Kentaro Yamaguchi§

*Contribution from the Department of Chemistry, Faculty of Science, Shizuoka University, 836 Ohya, Shizuoka 422-8529, Japan, Department of Chemistry, University of Tsukuba, Tsukuba, Ibaraki 305-8571, Japan, and Chemical Analysis Center, Chiba University, Inage-ku, Chiba 263-8522, Japan*

Received November 12, 2002; E-mail: skkobay@ipc.shizuoka.ac.jp

***Abstract:*** The crystal structures for three types of three-dimensional (3-D) hydrogen-bonded networks of hexakis(4-carbamoylphenyl)benzene (**1**), the network morphologies of which depend greatly on crystallization conditions, have been determined. When this compound is crystallized from hot DMSO, the resulting crystals, **1**·12DMSO (orthorhombic, $Pca2_1$), showed a 3-D hydrogen-bonded porous network (type A) via 1-D catemer chains as a hydrogen-bonding motif of six primary amide groups. The type A network creates chambers surrounded by six molecules of **1** and channels along the *c* axis to give the highest porosity among the network polymorphs of **1** investigated here. Crystallization from a boiling mixture of *n*-PrOH and water gave **1**·6*n*-PrOH (monoclinic, $P2_1/c$), which exhibits another type of 3-D hydrogen-bonded porous network (type B) via cyclic dimers as another hydrogen-bonding motif of six primary amide groups. The type B network leads to triangle-like channels along the *a* axis having a cross section of ca. 9.2 × 9.7 × 9.7 Å (including van der Waals radii). The crystal structure of **1**·$H_2O$ (monoclinic, $P2_1/c$), which was produced under hydrothermal conditions, showed a nonporous 3-D hydrogen-bonded network chain of amide groups (type C) composed of a mixed hydrogen bonding motif of helical catemer chains/cyclic dimer/catemer. Solvent-induced topological isomerism of these 3-D hydrogen-bonded networks of **1** arises from (i) the guest inclusion ability based on a radially functionalized hexagonal structure of **1**, (ii) the correlation between the hydrogen bond donor ability of the syn and anti protons of the primary amide group in host **1** and the hydrogen bond acceptor ability of the oxygen atoms of **1** and guest solvents, and (iii) the polarity of the bulk crystallization solvents.

## Introduction

Error correction through thermodynamic equilibration based on noncovalent interactions, minimization of synthetic efforts by use of modular subunits, and control of assembly processes through subunit design are characteristics of supramolecular approaches.[1] Self-assembly through directional and complementary noncovalent interactions such as hydrogen bonds and metal coordinations underlies crystal engineering (solid-state supramolecular chemistry) to achieve desirable molecular arrangements during the course of crystallization.[2] Particular attention has recently focused on the rational design of microporous solids based on supramolecular approaches because of the potential use of the resulting cavities and channels in nanotechnology, including shape- and size-selective molecular recognition,[3] adsorption, separation, storage,[4] catalysis,[5] and (opto)electronic applications.[6] However, the control of crystal and network structures in a predictable manner still remains an elusive task because of the delicate balance and competition between directional noncovalent interactions such as hydrogen

† Shizuoka University.
‡ University of Tsukuba.
§ Chiba University.

(1) (a) Lehn, J.-M. *Supramolecular Chemistry: Concepts and Perspectives*; VCH: Weinheim, Germany, 1995. (b) Leininger, S.; Olenyuk, B.; Stang, P. J. *Chem. Rev.* **2000**, *100*, 853−908. (c) Prins, L. J.; Reinhoudt, D. N.; Timmerman, P. *Angew. Chem., Int. Ed.* **2001**, *40*, 2382−2426.
(2) (a) Desiraju, G. R. *Crystal Engineering: The Design of Organic Solids*; Elsevier: Amsterdam, 1989. (b) Etter, M. C. *Acc. Chem. Res.* **1990**, *23*, 120−126. (c) Desiraju, G. R. *Angew. Chem., Int. Ed. Engl.* **1995**, *34*, 2311−2327. (d) *Comprehensive Supramolecular Chemistry, Solid-State Supramolecular Chemistry: Crystal Engineering*; MacNicol, D. D., Toda, F., Bishop, R., Eds.; Pergamon: New York, 1996; Vol. 6. (e) Zaworotko, M. J. *Chem. Commun.* **2001**, 1−9. (f) Steiner, T. *Angew. Chem., Int. Ed.* **2002**, *41*, 48−76.
(3) (a) Endo, K.; Sawaki, T.; Koyanagi, M.; Kobayashi, K.; Masuda, H.; Aoyama, Y. *J. Am. Chem. Soc.* **1995**, *117*, 8341−8352. (b) Holman, K. T.; Pivovar, A. M.; Swift, J. A.; Ward, M. D. *Acc. Chem. Res.* **2000**, *34*, 107−118.
(4) (a) Eddaoudi, M.; Moler, D. B.; Li, H.; Chen, B.; Reineke, T. M.; O'Keeffe, M.; Yaghi, O. M. *Acc. Chem. Res.* **2001**, *34*, 319−330. (b) Noro, S.; Kitagawa, S.; Kondo, M.; Seki, K. *Angew. Chem., Int. Ed.* **2000**, *39*, 2082−2084.
(5) (a) Fujita, M.; Kwon, Y. J.; Washizu, S.; Ogura, K. *J. Am. Chem. Soc.* **1994**, *116*, 1151−1152. (b) Endo, K.; Koike, T.; Sawaki, T.; Hayashida, O.; Masuda, H.; Aoyama, Y. *J. Am. Chem. Soc.* **1997**, *119*, 4117−4122. (c) Sawaki, T.; Endo, K.; Kobayashi, K.; Hayashida, O.; Aoyama, Y. *Bull. Chem. Soc. Jpn.* **1997**, *70*, 3075−3079. (d) Seo, J. S.; Whang, D.; Lee, H.; Jun, S. I.; Oh, J.; Jeon, Y. J.; Kim, K. *Nature* **2000**, *404*, 982−986.
(6) (a) *Organic Molecular Solids: Properties and Applications*; Jones, W., Ed.; CRC Press: Boca Raton, FL, 1997. (b) Thalladi, V. R.; Brasselet, S.; Weiss, H.-C.; Bläser, D.; Katz, A. K.; Carrell, H. L.; Boese, R.; Zyss, J.; Nangia, A.; Desiraju, G. R. *J. Am. Chem. Soc.* **1998**, *120*, 2563−2577. (c) Coronado, E.; Galán-Mascarós, J. R.; Gómez-García, C. J.; Laukhin, V. *Nature* **2000**, *408*, 447−449.

bonds and nondirectional noncovalent interactions such as van der Waals (dispersive) packing forces. The formation of hydrogen-bonded and/or metal coordination networks with large cavities often results in self-interpenetration to fill the voids in the initial host structure.[7]

Hydrogen-bonded networks have some advantages, due to soft and flexible properties. In some cases, the apohost, in which microporous hydrogen-bonded networks with channels are collapsed upon removal of guests due to crystal packing forces, could be reversibly restored to its original state concomitant with guest reinclusion in a stoichiometric manner when apohost crystals were exposed to liquid, gaseous, or solid guest molecules.[3a,8] Numerous strategies for designer organic host lattices based on hydrogen bonds have been explored. The introduction of sterically demanding substituents into trigonal molecules,[9] the use of macrocycles with multiple hydrogen-bonding sites,[10] the pillared layer system based on the combination of guanidinium and organodisulfonate ions,[3b,11] the bis(resorcinol) orthogonal aromatic triad system,[3a,8,12] and the steroid host system[13] have been intensively studied to prevent interpenetration of 2-D hydrogen-bonded porous networks. Recently, we have reported the 2-D hydrogen-bonded porous networks of hexakis(4-hydroxyphenyl)benzene and hexakis(4-carboxyphenyl)benzene (**2**).[14] These are highly symmetrical molecules that can bear six radial hydrogen-bonding sites and exhibit an orthogonal arrangement of the interactive groups with respect to the core moiety.[15,16]

One of the goals of crystal engineering is the construction of 3-D hydrogen-bonded porous networks without interpenetration, because 3-D hydrogen-bonded networks tend to be more susceptible to self-interpenetration than 2-D networks due to enlargement of the void space in the crystal lattice.[17] Our design for the extension of 2-D to 3-D hydrogen-bonded networks in hexaarylbenzene derivatives is to use a primary amide group in place of the carboxylic acid group: that is, hexakis(4-carbamoylphenyl)benzene (**1**). The most distinctive feature of the primary amide group is the presence of an *anti proton as well as a syn proton*, whereas the carboxylic acid group has either a syn or an anti proton. The primary amide group can adopt a variety of hydrogen-bonding motifs based on combinations of syn and anti protons on the nitrogen atom with syn and anti lone pairs of electrons on the oxygen atom.[18−20] Therefore, N−H anti protons of the hexakis(primary amide) host **1** would endow a 2-D hydrogen-bonded porous network of the hexakis(carboxylic acid) host **2**[14b] with the third dimension. Herein we report the synthesis and crystal structures of three types of 3-D hydrogen-bonded networks of hexakis(4-carbamoylphenyl)benzene (**1**) without self-interpenetration, in which a solvent-induced polymorphism of 3-D hydrogen-bonded networks of **1** is found.[21,22] The solvent-induced topological isomerism of 3-D hydrogen-bonded networks of **1** would result from the correlation between the hydrogen bond donor ability of the primary amide syn and anti protons of **1** and the hydrogen bond acceptor ability of the oxygen atoms of **1** and guest solvents,[23] as well as from a radially functionalized hexagonal structure of **1**.

## Results and Discussion

**Synthesis and Solubility of 1.** Hexakis(4-carbamoylphenyl)-benzene (**1**) was prepared by the two-phase reaction of hexakis-


(7) (a) Sharma, C. V. K.; Zaworotko, M. J. *Chem. Commun.* **1996**, 2655−2656. (b) Batten, S. R.; Robson, R. *Angew. Chem., Int. Ed. Engl.* **1998**, *37*, 1460−1494.
(8) Dewa, T.; Endo, K.; Aoyama, Y. *J. Am. Chem. Soc.* **1998**, *120*, 8933−8940.
(9) Kolotuchin, S. V.; Fenlon, E. E.; Wilson, S. R.; Loweth, C. J.; Zimmerman, S. C. *Angew. Chem., Int. Ed. Engl.* **1995**, *34*, 2654−2657.
(10) (a) Ghadiri, M. R.; Granja, J. R.; Milligan, R. A.; McRee, D. E.; Khazanovich, N. *Nature* **1993**, *366*, 324−327. (b) Venkataraman, D.; Lee, S.; Zhang, J.; Moore, J. S. *Nature* **1994**, *371*, 591−593. (c) MacGillivray, L. R.; Atwood, J. L. *J. Am. Chem. Soc.* **1997**, *119*, 6931−6932. (d) Kobayashi, K.; Shirasaka, T.; Horn, E.; Furukawa, N. *Tetrahedron Lett.* **1999**, *40*, 8883−8886. (e) Bong, D. T.; Clark, T. D.; Granja, J. R.; Ghadiri, M. R. *Angew. Chem., Int. Ed.* **2001**, *40*, 988−1011.
(11) (a) Russell, V. A.; Evans, C. C.; Li, W.; Ward, M. D. *Science* **1997**, *276*, 575−579. (b) Holman, K. T.; Martin, S. M.; Parker, D. P.; Ward, M. D. *J. Am. Chem. Soc.* **2001**, *123*, 4421−4431.
(12) (a) Kobayashi, K.; Endo, K.; Aoyama, Y.; Masuda, H. *Tetrahedron Lett.* **1993**, *34*, 7929−7932. (b) Kobayashi, K.; Koyanagi, M.; Endo, K.; Masuda, H.; Aoyama, Y. *Chem. Eur. J.* **1998**, *4*, 417−424.
(13) Sada, K.; Sugahara, M.; Kato, K.; Miyata, M. *J. Am. Chem. Soc.* **2001**, *123*, 4386-4392 and references therein.
(14) (a) Kobayashi, K.; Shirasaka, T.; Sato, A.; Horn, E.; Furukawa, N. *Angew. Chem., Int. Ed.* **1999**, *38*, 3483−3486. (b) Kobayashi, K.; Shirasaka, T.; Horn, E.; Furukawa, N. *Tetrahedron Lett.* **2000**, *41*, 89−93.
(15) For hexaarylbenzene derivatives, see: Watson, M. D.; Fechtenkötter, A.; Müllen, K. *Chem. Rev.* **2001**, *101*, 1267−1300.
(16) For the hexakis-host clathrates which are based on benzene rings hexa-substituted by flexible but bulky sidearms such as arylthio groups, see: MacNicol, D. D.; Downing, G. A. In *Comprehensive Supramolecular Chemistry, Solid-State Supramolecular Chemistry: Crystal Engineering*; MacNicol, D. D., Toda, F., Bishop, R., Eds.; Pergamon: New York, 1996; Vol. 6, pp 421−464.
(17) For 3-D hydrogen-bonded networks with self-interpenetration based on tetrahedral (diamondoid)-type and octahedral-type hosts, see: (a) Ermer, O. *J. Am. Chem. Soc.* **1988**, *110*, 3747−3754. (b) Ermer, O.; Lindenberg, L. *Helv. Chim. Acta* **1991**, *74*, 825−877. (c) Simard, M.; Su, D.; Wuest, J. D. *J. Am. Chem. Soc.* **1991**, *113*, 4696−4698. (d) Brunet, P.; Simard, M.; Wuest, J. D. *J. Am. Chem. Soc.* **1997**, *119*, 2737−2738. (e) Reddy, D. S.; Dewa, T.; Endo, K.; Aoyama, Y. *Angew. Chem., Int. Ed.* **2000**, *39*, 4266−4268. (f) Thaimattam, R.; Xue, F.; Sarma, J. A. R. P.; Mak, T. C. W.; Desiraju, G. R. *J. Am. Chem. Soc.* **2001**, *123*, 4432−4445. (g) Vaid, T. P.; Sydora, O. L.; Douthwaite, R. E.; Wolczanski, P. T.; Lobkovsky, E. B. *Chem. Commun.* **2001**, 1300−1301.
(18) For hydrogen-bonding motifs of the primary amide group, see: (a) Leiserowitz, L.; Schmidt, G. M. J. *J. Chem. Soc. A* **1969**, 2372−2382. (b) Blake, C. C. F.; Small, R. W. H. *Acta Crystallogr.* **1972**, *B28*, 2201−2206. (c) Cobbledick, R. E.; Small, R. W. H. *Acta Crystallogr.* **1972**, *B28*, 2893−2896. (d) Berkovitch-Yellin, Z.; Leiserowitz, L. *J. Am. Chem. Soc.* **1980**, *102*, 7677−7690. (e) Leiserowitz, L.; Hagler, A. T. *Proc. R. Soc. London* **1983**, *A388*, 133−175. (f) Aakeröy, C. B.; Beatty, A. M. *Chem. Commun.* **1998**, 1067−1068. (g) Edgar, R.; Schultz, T. M.; Rasmussen, F. B.; Feidenhans'l, R.; Leiserowitz, L. *J. Am. Chem. Soc.* **1999**, *121*, 632−637. (h) Kobko, N.; Paraskevas, L.; del Rio, E.; Dannenberg, J. J. *J. Am. Chem. Soc.* **2001**, *123*, 4348−4349.
(19) For hydrogen-bonding motifs of the secondary amide group, see: (a) Leiserowitz, L.; Tuval, M. *Acta Crystallogr.* **1978**, *B34*, 1230−1247. (b) Weinstein, S.; Leiserowitz, L.; Gil-Av, E. *J. Am. Chem. Soc.* **1980**, *102*, 2768−2772. (c) Garcia-Tellado, F.; Geib, S. J.; Goswami, S.; Hamilton, A. D. *J. Am. Chem. Soc.* **1991**, *113*, 9265−9269. (d) Reference 10a. (e) Fan, E.; Yang, J.; Geib, S. J.; Stoner, T. C.; Hopkins, M. D.; Hamilton, A. D. *J. Chem. Soc., Chem. Commun.* **1995**, 1251−1252. (f) Lewis, F. D.; Yang, J.-S.; Stern, C. L. *J. Am. Chem. Soc.* **1996**, *118*, 12029−12037. (g) Lightfoot, M. P.; Mair, F. S.; Pritchard, R. G.; Warren, J. E. *Chem. Commun.* **1999**, 1945−1946. (h) Nguyen, T. L.; Fowler, F. W.; Lauher, J. W. *J. Am. Chem. Soc.* **2001**, *123*, 11057−11064.
(20) For hydrogen-bonding motifs of the carboxylic acid group, see: (a) Leiserowitz, L. *Acta Crystallogr.* **1976**, *B32*, 775−802. (b) Berkovitch-Yellin, Z.; Leiserowitz, L. *J. Am. Chem. Soc.* **1982**, *104*, 4052−4064. (c) Reference 9. (d) Kuduva, S. S.; Craig, D. C.; Nangia, A.; Desiraju, G. R. *J. Am. Chem. Soc.* **1999**, *121*, 1936−1944. (e) Moorthy, J. N.; Natarajan, R.; Mal, P.; Venugopalan, P. *J. Am. Chem. Soc.* **2002**, *124*, 6530−6531.
(21) For supramolecular (architectural) isomerism in hydrogen-bonded networks, see: (a) Miyata, M.; Shibakami, M.; Chirachanchai, S.; Takemoto, K.; Kasai, N.; Miki, K. *Nature* **1990**, *343*, 446−447. (b) MacGillivray, L. R.; Reid, J. L.; Ripmeester, J. A. *Chem. Commun.* **2001**, 1034−1035. (c) Reference 11b. (d) Reference 17f. (e) Horner, M. J.; Holman, K. T.; Ward, M. D. *Angew. Chem., Int. Ed.* **2001**, *40*, 4045−4048.
(22) For supramolecular (architectural) isomerism in metal coordination networks, see: (a) Hennigar, T. L.; MacQuarrie, D. C.; Losier, P.; Rogers, R. D.; Zaworotko, M. J. *Angew. Chem., Int. Ed.* **1997**, *36*, 972−973. (b) Kasai, K.; Aoyagi, M.; Fujita, M. *J. Am. Chem. Soc.* **2000**, *122*, 2140−2141. (c) Bourne, S. A.; Lu, J.; Moulton, B.; Zaworotko, M. J. *Chem. Commun.* **2001**, 861−862.
(23) For correlation between donor and acceptor abilities in stronger and weaker hydrogen bonds, see: (a) Etter, M. C.; Panunto, T. W. *J. Am. Chem. Soc.* **1988**, *110*, 5896−5897. (b) Reference 2b. (c) Reference 20d. (d) Aakeröy, C. B.; Beatty, A. M.; Helfrich, B. A. *Angew. Chem., Int. Ed.* **2001**, *40*, 3240−3242.

(4-carboxyphenyl)benzene (**2**)[14b] with thionyl chloride in 1,2-dichloroethane in the presence of benzyltriethylammonium chloride as a phase transfer catalyst,[24] followed by the addition of ammonia gas to the resulting mixture (total yield 87%). As

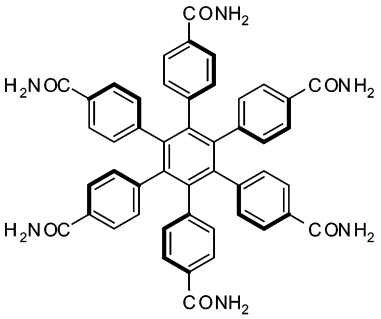


**1**

far as we have investigated, hexakis(primary amide) host **1** is slightly soluble in DMSO and DMF at room temperature, in a boiling mixture of $H_2O$ and *n*-PrOH (1:1), and under hydrothermal conditions, while being insoluble in $H_2O$, MeOH, EtOH, *n*-PrOH, and other common organic solvents even at boiling temperature. In this regard, **1** may be suitable as an organic zeolite.

**Crystallization and Molecular Structure of 1.** Crystallization by slowly cooling a solution of **1** (100 mg) in DMSO (30 mL) at 70 °C gave single crystals of **1**·12DMSO. Crystallization by slow cooling of a boiling solution of **1** (1 mg) in a 1:1 mixture of $H_2O$ and *n*-PrOH (20 mL) produced single crystals of **1**·6*n*-PrOH. Single crystals of **1** were also obtained under hydrothermal conditions.[25] A suspension of **1** (3 mg) in $H_2O$ (20 mL) in a 54 mL Teflon flask was placed in a stainless steel bomb, which was sealed and maintained in a convection oven at 170 °C for 48 h (ca. 0.94 MPa). When the bomb was cooled to 80 °C over a period of 9 h, maintained at this temperature for 15 h, and then cooled to room temperature over a period of 9 h, single crystals of **1**·$H_2O$ were obtained.[25] These crystals were used for collecting intensity data in the single-crystal X-ray diffraction analysis. Crystallographic data are summarized in Table 1.

The crystals of **1**·12DMSO (orthorhombic, $Pca2_1$), **1**·6*n*-PrOH (monoclinic, $P2_1/c$), and **1**·$H_2O$ (monoclinic, $P2_1/c$) gave different 3-D hydrogen-bonded networks (vide infra) and different conformational structures (Figure 1). For **1**·12DMSO and **1**·6*n*-PrOH, the asymmetric unit comprises the entire molecule. For **1**·$H_2O$, the unit cell contains two independent molecules in which each molecular structure has a center of symmetry (defined as **1a** and **1b**·$2H_2O$). The disposition of the amide oxygen atoms with respect to the central benzene core, the dihedral angles between the benzene arms of the benzamide moieties and the benzene core at C1−C6, and the dihedral angles between the benzene arms and the amide groups of O1−O6 are summarized in Table 2. In **1a**, two of the six benzene arms are twisted in the opposite direction with respect to the other four benzene arms twisted in the same direction. In **1b**, all of the benzene arms are twisted by 4−27° in the same direction with respect to the perpendicular direction to the benzene core.

(24) Burdett, K. A. *Synthesis* **1991**, 441−442.
(25) Ranganathan, A.; Pedireddi, V. R.; Rao, C. N. R. *J. Am. Chem. Soc.* **1999**, *121*, 1752−1753. The peculiar temperature and time profile of the present procedure was required to dissolve **1** in $H_2O$ and obtain single crystals suitable for the X-ray diffraction analysis.

***Table 1.*** Crystallographic Data for **1**·12DMSO, **1**·6*n*-PrOH, **1**·$H_2O$, and Benzamide

| | **1**·10DMSO[a] | **1**·6*n*-PrOH | **1**·$H_2O$ | benzamide[b] |
|---|---|---|---|---|
| formula | $C_{68}H_{96}N_6O_{16}S_{10}$ | $C_{66}H_{84}N_6O_{12}$ | $C_{48}H_{38}N_6O_7$ | $C_7H_7NO$ |
| fw | 1574.14 | 1153.42 | 810.86 | 121.14 |
| cryst syst | orthorhombic | monoclinic | monoclinic | monoclinic |
| space group | $Pca2_1$ | $P2_1/c$ | $P2_1/c$ | $P2_1/c$ |
| *a* (Å) | 25.270(2) | 11.522(2) | 16.120(4) | 5.5657(9) |
| *b* (Å) | 30.037(2) | 17.568(3) | 15.785(4) | 5.0353(9) |
| *c* (Å) | 10.0633(6) | 32.522(5) | 18.560(4) | 21.698(4) |
| α (deg) | 90 | 90 | 90 | 90 |
| *β* (deg) | 90 | 99.940(3) | 114.976(5) | 90.388(3) |
| *γ* (deg) | 90 | 90 | 90 | 90 |
| *V* (Å$^3$) | 7638.4(8) | 6484.6(15) | 4280.8(17) | 608.1(2) |
| *Z* | 4 | 4 | 4 | 4 |
| temp (K) | 123 | 120 | 103 | 173 |
| *R* | 0.092[c] | 0 087[d] | 0.081[d] | 0.038[d] |
| $R_w$[e] | 0.103 | 0.118 | 0.110 | 0.054 |
| GOF | 2.94 | 2.25 | 1.97 | 1.31 |

[a] Two molecules of DMSO could not be detected by X-ray diffraction analysis. The correct formula was **1**·12DMSO, which was confirmed by elemental analysis and thermogravimetric analysis (see text). [b] Crystallized from DMSO. [c] $R = \sum|F_o - F_c|/\sum F_o$ for $I > 2\sigma(I)$. [d] $R = \sum|F_o - F_c|/\sum F_o$ for $I > 3\sigma(I)$. [e] $R_w = [\sum w(F_o - F_c)^2/\sum wF_o^2]^{1/2}$.

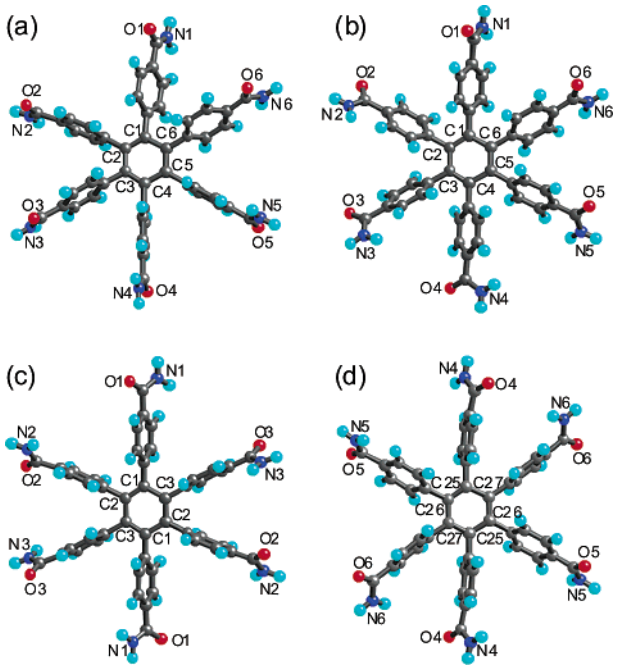


***Figure 1.*** Molecular structures of **1** in (a) **1**·12DMSO, (b) **1**·6*n*-PrOH, (c) **1a** in **1**·$H_2O$, and (d) **1b** in **1**·$H_2O$. Carbon, nitrogen, oxygen, and hydrogen atoms are shown in gray, blue, red, and light blue, respectively.

In **1**·6*n*-PrOH, all of the benzene arms are twisted by about 30° in the same direction with respect to the perpendicular direction to the benzene core. In **1**·12DMSO, the four benzene arms are almost perpendicular to the benzene core, while the other two benzene arms are twisted by approximately 25° in the same direction. Although the conformational asymmetry of **1** arising from the differences of dihedral angles between the respective six benzene arms and the benzene core makes this host chiral *R* or *S* for **1**·12DMSO and **1**·6*n*-PrOH, both enantiomers are alternately arranged along the hydrogen-bonded chains to give racemic crystals (vide infra).

**Hydrogen-Bonded Networks of Primary Amide Compounds.** The primary amide group can adopt a variety of hydrogen-bonding motifs based on combinations of syn and anti

***Table 2.*** Disposition of Amide Oxygen Atoms, Dihedral Angles between Benzene Core and Benzene Arms, and Dihedral Angles between Benzene Arms and Amide Groups in the Molecular Structure of **1**

Disposition of Amide O atoms of O1−O6 with Respect to Benzene Core

| | O1 | O2 | O3 | O4 | O5 | O6 |
|---|---|---|---|---|---|---|
| **1**·12DMSO | up | up | up | down | down | up |
| **1**·6*n*-PrOH | up | down | down | down | up | up |
| **1**·$H_2O$ | up | down | up[a]; | up | down | up[b] |

Dihedral Angles between Benzene Arms and Benzene Core at C1 to C6 (deg)

| | C1 | C2 | C3 | C4 | C5 | C6 |
|---|---|---|---|---|---|---|
| **1**·12DMSO | 66.1 | 91.5 | 95.0 | 90.3 | 89.2 | 64.7 |
| **1**·6*n*-PrOH | 61.1 | 58.6 | 64.4 | 60.6 | 64.7 | 59.3 |
| **1**·$H_2O$ | 78.1 | 83.1 | 99.7[a]; | 100.6 | 117.6 | 94.2[b,c] |

Dihedral Angles between Benzene Arms and Amide Group of O1−O6 (deg)

| | O1 | O2 | O3 | O4 | O5 | O6 |
|---|---|---|---|---|---|---|
| **1**·12DMSO | 4.7 | 1.9 | 9.4 | 8.6 | 10.1 | 11.9 |
| **1**·6*n*-PrOH | 8.8 | 8.5 | 25.1 | 28.6 | 15.6 | 2.7 |
| **1**·$H_2O$ | 28.9 | 31.8 | 27.2[a]; | 25.3 | 7.6 | 38.3[b] |

[a] O1−O3 for **1a**. [b] O4−O6 for **1b**. [c] C25−C27 for **1b**.

protons on the nitrogen atom with syn and anti lone pairs of electrons of the oxygen atom.[18,19] For example, the two-point interaction of the N−H syn proton with the syn lone pair of electrons of the oxygen atom forms a centrosymmetric cyclic dimer similar to that formed by the carboxylic acid group. In marked contrast to the cyclic dimer of a carboxylic acid, a cyclic dimer of a primary amide group can be extended to a ladder type of 1-D network tape by a translation motif or to a 2-D network sheet by a glide or a $2_1$ axis motif based on the interaction of the N−H anti proton with the anti lone pair of electrons of the oxygen atom. The one-point interaction of the N−H anti proton with the anti lone pair of electrons of the oxygen atom forms a catemer, which can also be extended to a 1-D catemer chain by a glide or a $2_1$ axis motif. Occasionally, the one-point interaction of the N−H syn proton with the syn lone pair of electrons of the oxygen atom gives a 1-D catemer chain by a helical $2_1$ axis motif.[26] In general, the selectivity for hydrogen-bonding patterns in the primary amide group appears to be governed by the inherent molecular structure. Benzamide persistently forms a 1-D network tape by a translation motif of a cyclic dimer, the formation of which is independent of crystallization solvents such as DMSO,[27] alcohols,[18g] and benzene.[18b] Terephthalamide forms a 2-D hydrogen-bonded sheet by 2-fold translation motifs of the cyclic dimer of the benzamide moiety.[18c]

The hexakis(primary amide) host **1** has six benzamide moieties radially connected to the central benzene core. We initially anticipated that **1** might lead to a 3-D hydrogen-bonded porous network by 6-fold translation motifs of the cyclic dimer of the benzamide moiety. However, this network has not yet been observed, probably due to steric repulsion between hosts. Instead, we found another three types of 3-D hydrogen-bonded networks of **1**, the network morphology of which is isomerized, depending strongly on crystallization conditions as well as on the solvent guest molecules. The 3-D hydrogen-bonded network structures, hydrogen-bonding motifs, hydrogen-bonding distances, and network porosity for the crystals of **1**·12DMSO (type A), **1**·6*n*-PrOH (type B), and **1**·$H_2O$ (type C) are summarized in Figure 2 and Table 3.

**Hydrogen-Bonded Network of 1·12DMSO.** The crystals of **1**·12DMSO showed a 3-D hydrogen-bonded porous network of type A via 1-D catemer chains based on the one-point interaction of the N−H anti protons with the anti lone pairs of electrons on the oxygen atoms in the six primary amide groups (Figures 2a, 3, and 4).[18,19]

In the *ab* plane, the hexakis(primary amide) hosts **1** do not hydrogen bond to each other (2-D non-hydrogen-bonded porous sheet), although a large space is provided by four molecules of **1**. The center−center interbenzene core distance along the *a* axis is 25.3 Å, and the intermolecular amide−amide distance along the *b* axis is 15.0 Å (Figure 3a). The adjacent 2-D non-hydrogen-bonded porous sheets, which are translated by 15.0 Å along the *b* axis, are layered in an offset manner (ABAB pattern) and are linked by six kinds of 1-D catemer chains along the *c* axis to give a 3-D hydrogen-bonded porous network of type A without self-interpenetration (Figure 3b). The six catemer chains are each composed of the same group number among six amide groups of host **1**: namely, the catemer chain of H1 consists of only amide group 1 assigned in Figure 1a. One molecule of host **1** hydrogen bonds to eight nearest neighbors via catemer chains H1−H6: in other words, assembly of six molecules of **1** makes one chamber (Figure 3e). The hydrogen-bonding distances of N1···O1, N2···O2, N3···O3, N4···O4, N5···O5, and N6···O6 for catemer chains H1−H6 are 2.96, 2.81, 2.92, 2.87, 2.89, and 2.92 Å, respectively (Table 3). The catemer chains of H1, H2, H4, and H5 are glide motifs, whereas those of H3 and H6 are $2_1$ axis motifs.

The detailed 3-D packing structure is shown in parts b−d of Figure 3. The front view shows two types of channels along the *c* axis (Figure 3b). The moieties marked on the front view are defined as the first row and the first column. The top view of the first row of the front view, as viewed down the *ac* plane, indicates that catemer chains H1 and H2 are antiparallel to H4

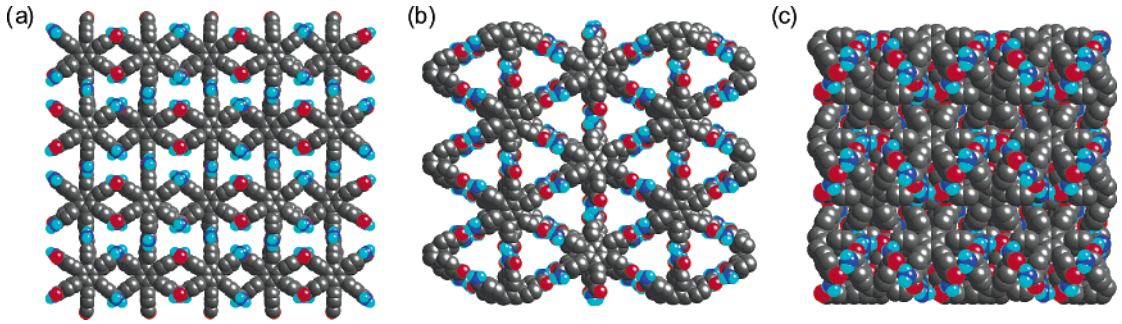


***Figure 2.*** Space-filling representation for 3-D hydrogen-bonded networks in the crystal structures of (a) **1**·12DMSO of type A, (b) **1**·6*n*-PrOH of type B, and (c) **1**·$H_2O$ of type C. Guest solvents and hydrogen atoms except for $NH_2$ protons of the primary amide group are omitted for clarity.

***Table 3.*** Hydrogen-Bonding Motif, Property of Network Dimension, Hydrogen-Bonding Distances, and Network Porosity for Crystals of **1**·12DMSO, **1**·6*n*-PrOH, **1**·$H_2O$, and Benzamide

| | **1**·12DMSO | **1**·6*n*-PrOH | **1**·$H_2O$[a] | benzamide[b] |
|---|---|---|---|---|
| H-bonding motif | catemer chain | cyclic dimer | helical catemer chain/ cyclic dimer/catemer | cyclic dimer/ translation |
| property of network dimension | 3-D porous | 3-D porous | 3-D nonporous | 1-D tape |
| amide−amide H-bonding dist (Å) | N1···O1 = 2.962(8)<br>N2···O2 = 2.810(8)<br>N3···O3 = 2.920(9)<br>N4···O4 = 2.869(8)<br>N5···O5 = 2.887(9)<br>N6···O6 = 2.922(8) | N1···O3 = 2.961(5)<br>N3···O1 = 2.851(6)<br>N4···O6 = 3.003(5)<br>N6···O4 = 2.855(5)<br>N2···O2 = 2.886(5)<br>N5···O5 = 2.876(5) | N1···O1 = 2.914(8)<br>N1···O2 = 2.885(9)<br>N2···O3 = 2.864(8)<br>N3···O1 = 2.947(8)<br>N4···O6 = 2.830(8)<br>N5···O5 = 2.947(8)<br>N3···O4 = 2.823(8)<br>N5···O3 = 2.814(7) | N1···O1 = 2.905(1)<br>N1···O1 = 2.9434(13) |
| amide−solvent H-bonding dist (Å) | N1···O15 = 2.837(9)<br>N2···O8 = 2.960(8)<br>N3···O9 = 2.912(8)<br>N4···O10 = 2.910(8)<br>N5···O13 = 2.901(9)<br>N6···O14 = 2.953(8) | N1···O7 = 2.944(6)<br>N2···O9 = 2.894(6)<br>N3···O10 = 2.948(6)<br>N4···O12 = 2.934(8)<br>N5···O11 = 3.259(9)<br>N6···O8 = 2.955(6)<br>O3···O8 = 2.669(5)<br>O4···O7 = 2.717(5)<br>O6···O10 = 2.703(5) | N6···O7 = 2.819(9)<br>O4···O7 = 2.784(7)<br>O5···O7 = 2.777(7) | |
| solvent−solvent H-bonding dist (Å) | | O9···O11 = 2.676(8)<br>O10···O12 = 3.040(10)<br>O11···O12 = 3.18(1) | | |
| packing coefficient (%)[c] | 35.8 | 42.1 | 63.8 | 74.6 |
| pore size (mL/g)[c] | 0.931 | 0.712 | 0.294 | 0.192 |

[a] O1−O3 and N1−N3 belong to **1a**, and O4−O6 and N4−N6 belong to **1b**. [b] Crystallized from DMSO. [c] See refs 3a and 28.

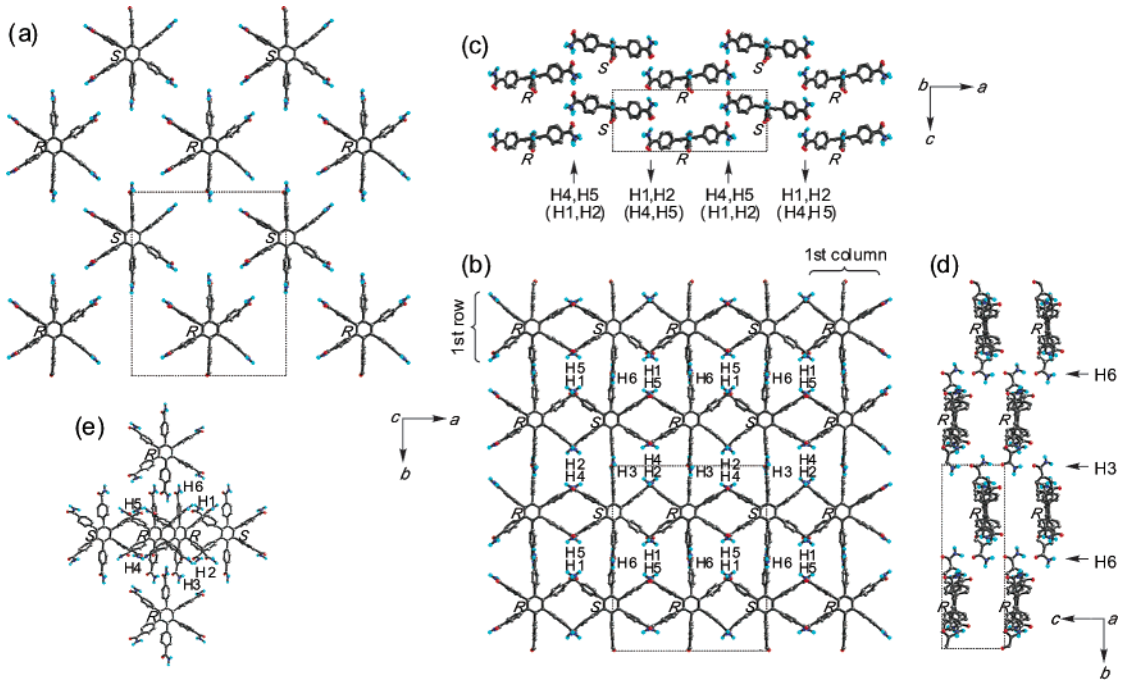


***Figure 3.*** Crystal structure of **1**·12DMSO: (a) 2-D non-hydrogen-bonded sheet as viewed down the *ab* plane; (b) front view of the 3-D hydrogen-bonded network as viewed down the *ab* plane (packing arrangement of four 2-D sheets); (c) top view toward the first row of the front view as seen down the *ac* plane; (d) side view toward the first column of the front view as seen down the *bc* plane; (e) molecular arrangement in one chamber. DMSO molecules and hydrogen atoms except for $NH_2$ protons of the primary amide group are omitted for clarity.

and H5 along the *c* axis and the network is composed of both enantiomers *R* and *S* (Figure 3c). This porous network gives a chamber of 10.1 × 12.6 Å, but no channel, because the second row of the front view is translated by a half period along the *c* axis with respect to the first row. The side view of the first column of the front view, as seen down the *bc* plane, indicates that catemer chains H3 and H6 are parallel to the *c* axis and the network is composed of either enantiomer *R* or *S* (Figure 3d). This porous network also gives a chamber of 10.1 × 15.0 Å, but no channel, because the second column of the front view is also translated by a half period along the *c* axis with respect to the first column. Thus, the 3-D hydrogen-bonded porous network of type A in **1**·12DMSO produces chambers surrounded

(26) For helical network motif of primary amides: (a) Long, R. E.; Maddox, H.; Trueblood, K. N. *Acta Crystallogr.* **1969**, *B25*, 2083−2094. (b) References 18d,e and references therein.
(27) This work.

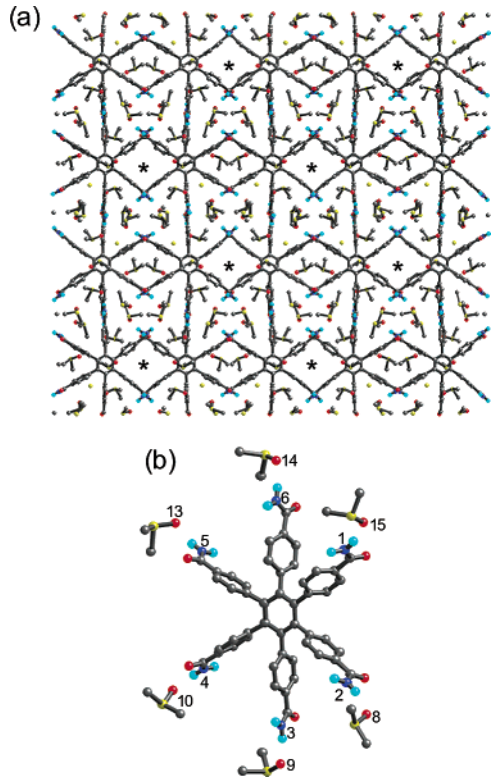


***Figure 4.*** (a) Packing diagram and (b) hydrogen-bonding pattern of **1** with DMSO in the crystal structure of **1**·12DMSO. Hydrogen atoms except for $NH_2$ protons of the primary amide group of **1** are omitted for clarity. The empty space marked by an asterisk in Figure 4a should be filled by two molecules of non-hydrogen-bonded DMSO, although they could not be detected by X-ray diffraction analysis.

by six molecules of **1** (Figure 3e) and two types of channels along the *c* axis to give the highest porosity among the network morphologies of **1** presented in this work (Figure 2a and Table 3). The packing coefficient and pore size of host **1** in **1**·12DMSO, namely the ratio of the host volume with respect to the total volume of the unit cell, and the volume of empty space per gram of the host, are 35.8% and 0.931 mL/g, respectively.[28] These values indicate that the 3-D hydrogen-bonded network of hexakis(4-carbamoylphenyl)benzene (**1**) is more porous than the 2-D hydrogen-bonded networks of hexakis(4-carboxyphenyl)benzene (**2**).[14b] The packing coefficient and pore size of **2** in **2**·2(2,7-dimethoxynaphthalene) are 43.0% and 0.661 mL/g, respectively.[14b]

Twelve molecules of DMSO per molecule of **1** are included in the crystal lattice. The packing diagram and hydrogen-bonding pattern of **1** with DMSO are shown in Figure 4. Six of the 12 included DMSO molecules are hydrogen-bonded to the N−H syn protons of the six amide groups of **1** with N···O distances of 2.84−2.96 Å (Figure 4b and Table 3), whereas the six N−H anti protons of **1** participate in the 3-D hydrogen-bonded porous network of type A. The other six molecules of DMSO do not hydrogen bond to **1** and are highly disordered, and two molecules of DMSO could not be detected by the X-ray diffraction analysis. The correct stoichiometry of **1**:DMSO = 1:12 was determined by elemental analysis and thermogravimetric analysis. The loss of two and four molecules of DMSO was observed by 97 and 182 °C, respectively, indicating six molecules of non-hydrogen-bonded DMSO (Figure 5). The loss of six molecules of hydrogen-bonded DMSO started at around 335 °C.

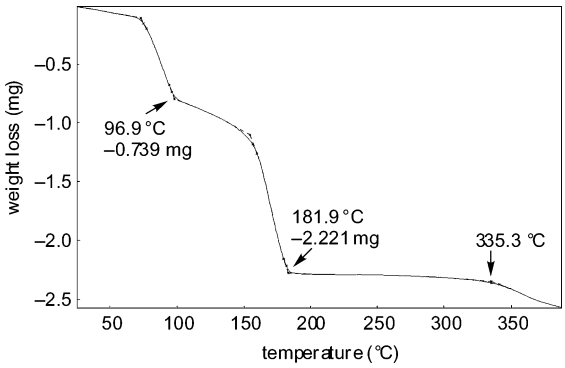


***Figure 5.*** Trace of thermogravimetric analysis of **1**·12DMSO at a heating rate of 5 °C $min^{-1}$.

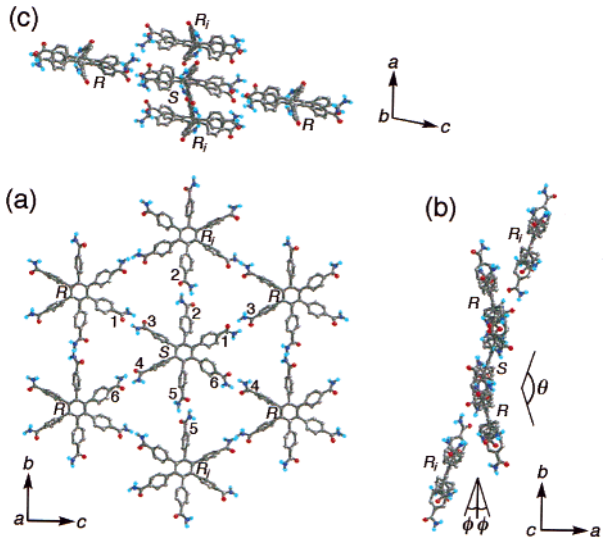


***Figure 6.*** One host molecule with nearest hydrogen-bonded neighbors in the crystal structure of **1**·6*n*-PrOH: (a) front view as seen down along the *a* axis; (b) side view as seen down along the *c* axis; (c) top view as seen down along the *b* axis. *n*-PrOH molecules and hydrogen atoms except for $NH_2$ protons of the primary amide group are omitted for clarity.

**Hydrogen-Bonded Network of 1·6*n*-PrOH.** The crystals of **1**·6*n*-PrOH showed another type of 3-D hydrogen-bonded porous network of type B via cyclic dimers based on the two-point interaction of the N−H syn protons with the syn lone pairs of electrons of the oxygen atoms in the six primary amide groups (Figures 2b and 6−8).[18]

One molecule of host **1** hydrogen bonds to six nearest neighbors via six cyclic dimers of the primary amide groups (Figure 6). The hydrogen-bonding distances of N1···O3, N3···O1, N4···O6, N6···O4, N2···O2, and N5···O5 are 2.96, 2.85, 3.00, 2.86, 2.89, and 2.88 Å, respectively (Table 3). Four peripheral molecules of the *R* enantiomer hydrogen bond to the central molecule of the *S* enantiomer via two kinds of cyclic dimers between amide groups 1 and 3 and between amide groups 4 and 6 to form a 2-D hydrogen-bonded puckered network sheet with respect to the *bc* plane (Figure 6a), wherein the puckering angle of the benzene cores with respect to the *bc*

(28) The packing coefficient of the host ($K_h$) was calculated as $(V_hZ_h)/V_c$, where $V_h$ is the calculated molecular volume of the host, $Z_h$ is the number of hosts in the unit cell, and $V_c$ is the total volume of the unit cell (see also ref 3a). The pore size of the host was calculated as $(1 - K_h)/d_h$, where $d_h = \{((MW_h)Z_h)/(6.02 \times 10^{23})\}/(V_c \times 10^{-24})$ and $MW_h$ is the molecular weight of the host. The $V_h$ value was calculated with Hyperchem Pro 6.0 as the software and QSAR properties as a module.

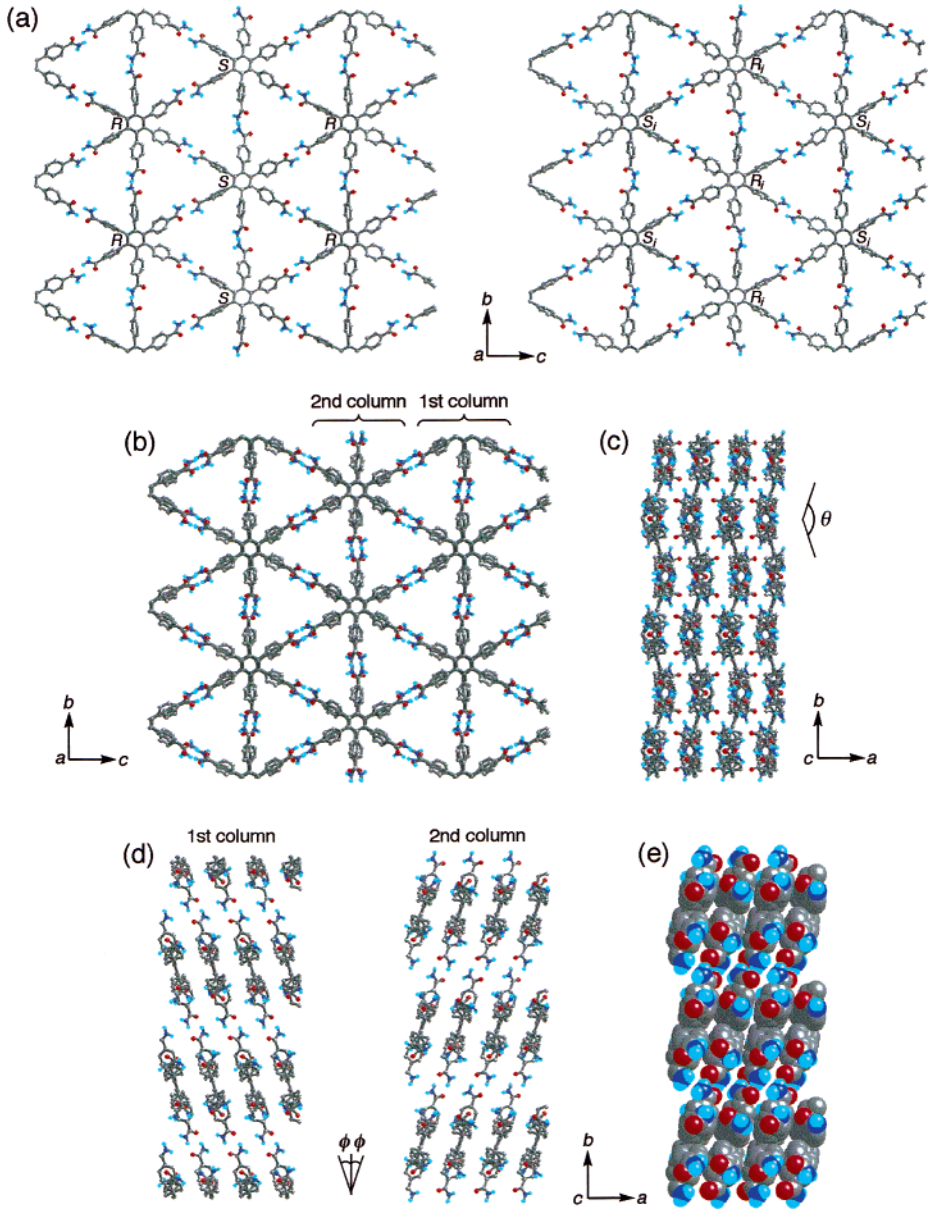


***Figure 7.*** Crystal structure of **1**·6*n*-PrOH: (a) front views of one 2-D hydrogen-bonded sheet and adjacent sheet as viewed down along the *a* axis; (b) front view of the 3-D hydrogen-bonded network as viewed down along the *a* axis (packing arrangement of four 2-D sheets); (c) side view of the 3-D network as viewed down along the *c* axis; (d) side views of the first and second columns defined in Figure 7b as viewed down along the *c* axis; (e) space-filling representation of the side view of the second column. *n*-PrOH molecules and hydrogen atoms except for the $NH_2$ protons of the primary amide group are omitted for clarity.

plane is $\theta = 143.6°$ (Figure 6b). The other two peripheral molecules of $R_i$ (i means an inversion) do not belong to this network sheet (Figure 6b,c) and hydrogen bond to the central molecule of *S* via two kinds of cyclic dimers between amide group 2 of *S* and group 2 of $R_i$ and between amide group 5 of *S* and group 5 of $R_i$ to form a 1-D hydrogen-bonded network tape parallel to the *ab* plane. The two molecules of $R_i$ belong to the neighboring sheets above and below. Thus, enantiomer *S* hydrogen bonds to four *R* enantiomers in a 2-D racemic sheet and to two $R_i$ enantiomers in a 1-D racemic tape.

One 2-D racemic sheet is composed of enantiomers *R* and *S*, whereas the adjacent 2-D racemic sheet is composed of $R_i$ and $S_i$ (Figure 7a). These 2-D hydrogen-bonded puckered porous sheets with respect to the *bc* plane are stacked along the *a* axis without translation (Figure 7b). Furthermore, the stacked 2-D sheets are linked to each other by the 1-D hydrogen-bonded tapes parallel to the *ab* plane (Figure 7c,d) to be assembled into the 3-D hydrogen-bonded porous network of type B (Figures 2b and 7b). When the moieties marked on the front view of Figure 7b are defined as the first and second columns, the side views of those indicate that the 1-D tapes in each column are stacked against each other by edge-to-face aromatic $\pi-\pi$ interactions between benzene arms and that the 1-D tapes in the first and second columns are alternately tilted by $\phi = \pm 18.2°$ with respect to the *b* axis (Figure 7d,e). This is due to the 2-D puckered sheets with respect to the *bc* plane. The center−center interbenzene core distance (tape-to-tape distance) along the *a* axis is 5.8 Å (Figure 7d), and the center−center interbenzene core distances in the 2-D puckered sheet are 17.6 and 18.5 Å (Figure 7b). Thus, the 3-D hydrogen-bonded porous network of type B in **1**·6*n*-PrOH leads to triangle-like channels along the *a* axis with a cross-section of ca. 9.2 × 9.7 × 9.7 Å,

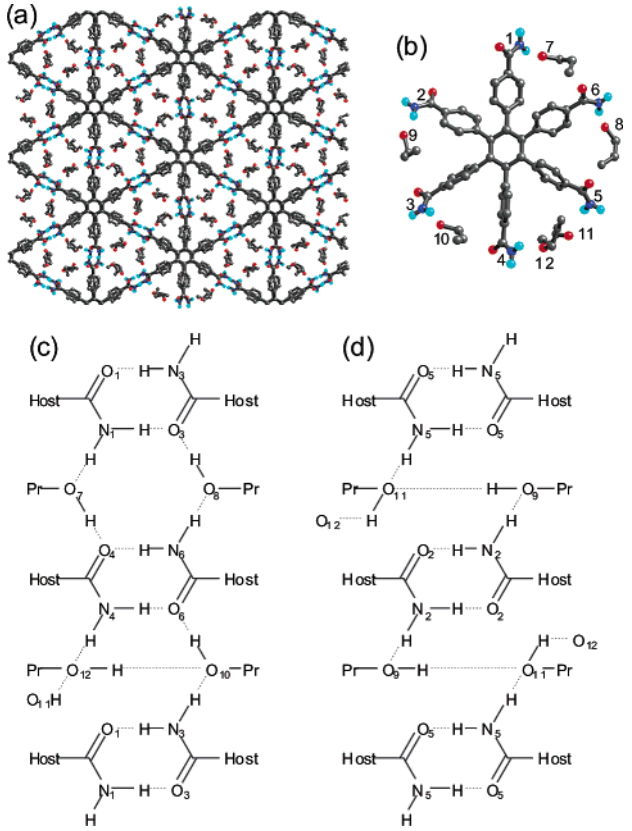


***Figure 8.*** (a) Packing diagram and (b) hydrogen-bonding pattern of **1** with *n*-PrOH in the crystal structure of **1**·6*n*-PrOH. Hydrogen atoms except for the $NH_2$ protons of the primary amide group of **1** are omitted for clarity. Schematic representations of the hydrogen-bonding patterns of **1** with *n*-PrOH (c) between the neighboring 2-D sheets and (d) between the neighboring 1-D tapes.

including van der Waals radii (Figure 2b). There are no channels and no spaces in the other directions. The porosity based on the packing coefficient (42.1%) and pore size (0.712 mL/g) of host **1** in **1**·6*n*-PrOH is smaller than that in **1**·12DMSO (Table 3).

The packing diagram and hydrogen-bonding pattern of **1** with *n*-PrOH are shown in Figure 8. All of the six included *n*-PrOH molecules hydrogen bond to the N−H anti protons of the six amide groups of **1** and are accommodated in the channel of **1** (Figure 8a,b). The hydrogen-bonding N···O distances (Å) are N1···O7 = 2.94, N2···O9 = 2.89, N3···O10 = 2.95, N4···O12 = 2.93, N5···O11 = 3.26,[29] and N6···O8 = 2.96 (Table 3). Three of the four *n*-PrOH molecules hydrogen-bonded to the 2-D sheet composed of amide groups 1, 3, 4, and 6, namely *n*-PrO7H, *n*-PrO8H, and *n*-PrO10H, serve as a hydrogen-bonded connector between the neighboring 2-D sheets to stabilize the 3-D network (Figure 8c).[29]

**Hydrogen-Bonded Network of 1·$H_2O$.** The crystals of **1**·$H_2O$ exhibited a nonporous 3-D hydrogen-bonded network chain of amide groups (type C) composed of a mixed hydrogen-bonding motif of helical catemer chains/cyclic dimer/catemer

(29) The hydrogen bond of the *n*-PrO11H with the N5−H anti proton of amide group 5 is very weak (the N5···O11 distance is 3.26 Å) because the *n*-PrO11H hydrogen bonds tightly to the *n*-PrO9H with an O9···O11 distance of 2.68 Å (Figure 8d). The interatomic distance of O1···O12 (3.43 Å) is too long to make a hydrogen bond, because the *n*-PrO12H group hydrogen-bonds to both the *n*-PrO10H and the *n*-PrO11H groups with O···O distances of 3.04 and 3.18 Å, respectively (Figure 8c,d). Thus, there is a hydrogen-bonding chain of O10···O12···O11···O9 among the included guest molecules in the channel of **1**.

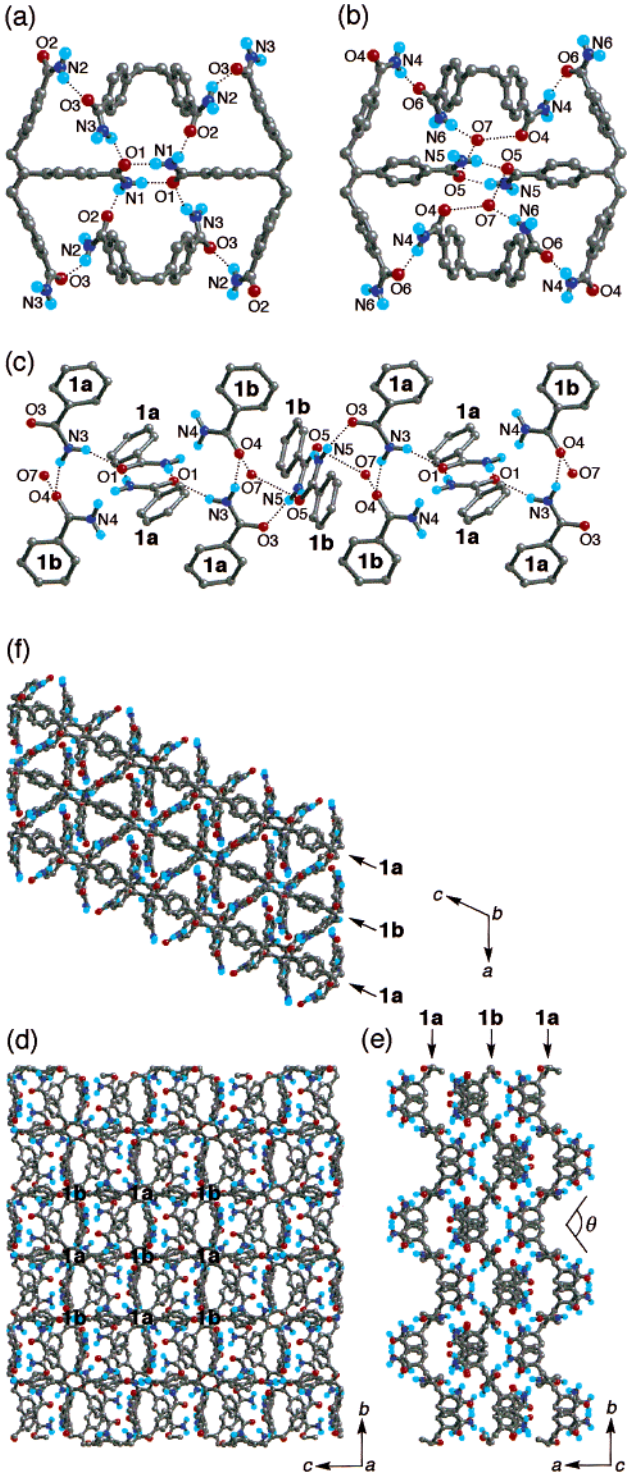


***Figure 9.*** Crystal structure of **1**·$H_2O$: fundamental hydrogen-bonding patterns of (a) **1a** (amide groups 1−3), (b) **1b**·2$H_2O$ (amide groups 4−6), and (c) **1a** with **1b**·2$H_2O$; 3-D hydrogen-bonded network of (d) front view as seen down along the *a* axis, (e) side view as seen down along the *c* axis, and (f) top view as seen down along the *b* axis. Hydrogen atoms except for the $NH_2$ protons of the primary amide group of **1** are omitted for clarity.

(Figures 2c and 9−11). The unit cell contains two independent molecules in which each molecular structure has a center of symmetry (defined as **1a** and **1b**·2$H_2O$).

The fundamental hydrogen-bonding patterns of **1a** (amide groups 1−3), **1b**·2$H_2O$ (amide groups 4−6), and **1a** with **1b**·2$H_2O$ are shown in Figure 9. A 2-D hydrogen-bonded

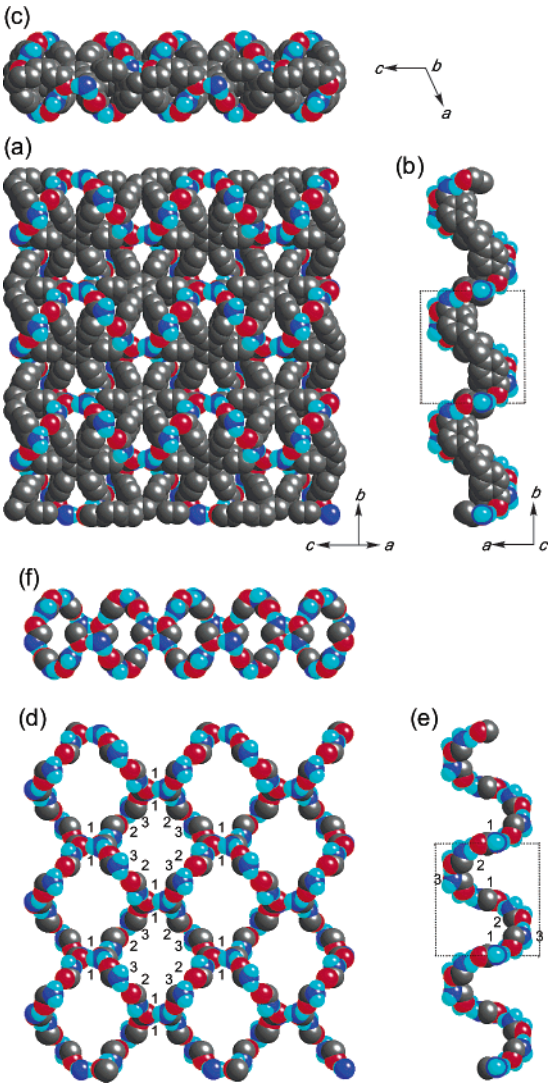


***Figure 10.*** Space-filling representation of 2-D hydrogen-bonded sheet of **1a** in the crystal structure of **1**·$H_2O$: (a) front view as seen down the *bc* plane; (b) side view as seen down along the *c* axis; (c) top view as seen down along the *b* axis. Hydrogen atoms, except for $NH_2$ protons of the primary amide group of **1a**, are omitted for clarity. 2-D hydrogen-bonded network chain of **1a**, wherein only amide groups are represented for clarity: views of d−f correspond to a−c, respectively.

network of **1a** alone is composed of one cyclic dimer with an N1···O1 distance of 2.91 Å and three catemers with N1···O2, N2···O3, and N3···O1 distances of 2.89, 2.86, and 2.95 Å, respectively (Figure 9a and Table 3). The combination of one molecule of **1b** and two molecules of $H_2O7$ also gives a 2-D hydrogen-bonded network via one cyclic dimer with an N5···O5 distance of 2.95 Å, one catemer with an N4···O6 distance of 2.83 Å, and three-point hydrogen bonds of the interposed $H_2O7$ with three amide groups with O4···O7, O5···O7, and N6···O7 distances of 2.78, 2.78, and 2.82 Å, respectively (Figure 9b). The hydrogen bonds of **1a** with **1b** are based on two catemers with N3···O4 (N−H syn proton) and N5···O3 (N−H anti proton) distances of 2.82 and 2.81 Å, respectively (Figure 9c). Thus, the 2-D networks of **1a** and **1b**·$2H_2O$ are alternately assembled into a nonporous 3-D hydrogen-bonded network chain of amide groups (Figures 2c and 9d−f). The packing coefficient and pore size of host **1** in **1**·$H_2O$ are 63.8% and 0.294 mL/g, respectively (Table 3). The respective 2-D hydrogen-bonded networks of **1a** and **1b**·$2H_2O$

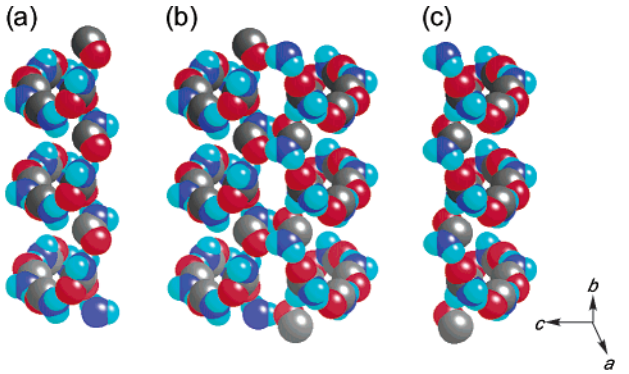


***Figure 11.*** 1-D hydrogen-bonded helical network chain of **1a** in the crystal structure of **1**·$H_2O$, wherein only amide groups are represented for clarity: (a) *P*-helical catemer chain; (b) assembly of antiparallel *P*- and *M*-helical catemer chains; (c) antiparallel *M*-helical catemer chain.

form puckered sheets with respect to the *bc* plane, wherein the puckering angles of the benzene cores of **1a** and **1b** with respect to the *bc* plane are the same, ca. $\theta = 108°$ (Figure 9e).

Parts a−c of Figure 10 show one 2-D puckered sheet of **1a** represented by a space-filling model. This structure is nonporous but seems to have a helical network chain of amide groups, which becomes clear when particular attention is focused on only the amide groups, as shown in Figures 10d−f and 11. The 2-D hydrogen-bonded network chain of amide groups (Figures 10d−f) is composed of antiparallel left-handed *M*- and right-handed *P*-helical 1-D catemer chains along the *b* axis in which only the N−H anti protons of the amide groups are involved (Figure 11). The helical turn repeats every six amide groups composed of three molecules of **1a** and is 15.8 Å by a $6_1$-screw axis (Figures 10d,e and 11). The antiparallel *M*- and *P*-helical 1-D catemer chains of **1a** are assembled alternately into the 2-D network chain via cyclic dimers of amide group 1 (Figures 10d and 11). In general, the N−H syn proton and the O−H syn proton participate in the helical 1-D networks of primary amides,[26] cyclic secondary amides,[18d] and carboxylic acids,[20e] respectively. In marked contrast, only the N−H anti protons are involved in the helical 1-D catemer chains of **1a**. The helical networks in some bis- and tris(secondary amides) adopt the N−H anti proton.[30−32] The 2-D hydrogen-bonded network chain of **1b**·$2H_2O$ is also composed of antiparallel *M*- and *P*-helical 1-D catemer chains similar to those of **1a** by the interposition of a hydrogen-bonding water molecule.

**Factors for Solvent-Induced Polymorphism of 3-D Hydrogen-Bonded Networks of 1.** The 3-D hydrogen-bonded networks of type A in **1**·12DMSO, type B in **1**·6*n*-PrOH, and type C in **1**·$H_2O$ are composed of only catemer chains, only

(30) For the helical network motif of secondary amides using the N−H anti proton, see: (a) Geib, S. J.; Vicent, C.; Fan, E.; Hamilton, A. D. *Angew. Chem., Int. Ed. Engl.* **1993**, *32*, 119−121. (b) Reference 19g.

(31) For other helical hydrogen-bonded network motifs of hosts without chiral centers, see: (a) Hollingsworth, M. D.; Harris, K. D. M. In *Comprehensive Supramolecular Chemistry, Solid-State Supramolecular Chemistry: Crystal Engineering*; MacNicol, D. D., Toda, F., Bishop, R., Eds.; Pergamon: New York, 1996; Vol. 6, pp 177−237. (b) Allen, W. E.; Fowler, C. J.; Lynch, V. M.; Sessler, J. L. *Chem. Eur. J.* **2001**, *7*, 721−729.

(32) For other helical hydrogen-bonded network motifs of hosts with chiral centers, see: (a) Ung, A. T.; Gizachew, D.; Bishop, R.; Scudder, M. L.; Dance, I. G.; Craig, D. C. *J. Am. Chem. Soc.* **1995**, *117*, 8745−8756. (b) Hirschberg, J. H. K. K.; Brunsveld, L.; Ramzi, A.; Vekemans, J. A. J. M.; Sijbesma, R. P.; Meijer, E. W. *Nature* **2000**, *407*, 167−170. (c) Moriuchi, T.; Nomoto, A.; Yoshida, K.; Ogawa, A.; Hirao, T. *J. Am. Chem. Soc.* **2001**, *123*, 68−75. (d) Radhakrishnan, T. P.; Gangopadhyay, P. *Angew. Chem., Int. Ed.* **2001**, *40*, 2451−2455. (e) Custelcean, R.; Ward, M. D. *Angew. Chem., Int. Ed.* **2002**, *41*, 1724−1728.

cyclic dimers, and a mixed type of helical catemer chains/cyclic dimer/catemer, respectively, as hydrogen-bonding motifs of primary amide groups (Figure 2). All of the 3-D hydrogen-bonded networks of types A−C are formed without self-interpenetration. The solvent-induced topological isomerism[21,22] of these 3-D hydrogen-bonded networks of the hexakis(primary amide) host **1** arises from three factors.

The first factor is attributed to the radially functionalized hexagonal structure of **1**. Benzamide persistently forms a 1-D network tape by a translation motif of a cyclic dimer, the formation of which is independent of crystallization solvents such as DMSO,[27] *n*-PrOH,[18g] and benzene.[18b] No solvent molecules as a guest are included in the crystal lattice of benzamide. The packing coefficient of 74.6% of benzamide crystallized from DMSO is higher than the 35.8∼63.8% of **1** (Table 3). In marked contrast to benzamide, both the hydrogen-bonding motif and the 3-D hydrogen-bonded network morphology in **1** isomerize, depending on the crystallization solvents. The hexakis(primary amide) host **1** possesses the radially functionalized hexagonal structure, which can provide the crystal lattice with a cavity or a channel to accommodate guest solvents and have moderate flexibility of the dihedral angles between the respective benzene arms and the benzene core (Table 2) that can undergo induced-fit adjustment to guest solvents. Therefore, in the host **1** that can accommodate guest solvents into the network cavity, the properties of guest solvents would strongly affect the hydrogen-bonding motif and network morphology of **1** much more than those of benzamide.

The second factor is attributed to the correlation between the hydrogen bond donor ability of the syn and anti protons of the primary amide group in host **1** and the hydrogen bond acceptor ability of the oxygen atoms of **1** and guest solvents. It is known that the strongest donor hydrogen bonds to the strongest acceptor, while the weaker donor hydrogen bonds to the weaker acceptor.[23] Abraham et al. presented hydrogen bond structural constants that estimate the ability of functional groups to act as hydrogen bond acids and bases.[33] On the basis of the reported data, the sB scale indicating hydrogen bond basicity (the reported value is presented in parentheses), namely acceptor ability, increases in the order primary alcohol-*O*H (0.48)[34] < aromatic-C*O*NH$_2$ (0.53) < aliphatic-S*O*CH$_3$ (0.97), and the sA scale indicating hydrogen bond acidity, namely donor ability, increases in the order aliphatic-SOC*H*$_3$ (0.00) ≪ primary alcohol-O*H* (0.37)[34] < aromatic-CON*H*$_2$ (0.49).[33] Thus, the oxygen atom of DMSO and the N−H proton(s) of the primary amide group of **1** would be the strongest hydrogen bond acceptor and donor, respectively, in our system. Unfortunately, there are no data on which N−H proton of the primary amide group is the stronger donor, the N−H syn or anti proton. If the assumption that the N−H syn proton is a stronger donor than the N−H anti proton is true, the solvent-induced topological isomerism of 3-D hydrogen-bonded networks of **1** can be explained as follows. In the crystal structure of **1**·12DMSO, the N−H syn proton of the primary amide group of **1** as the stronger donor forms a hydrogen bond to the oxygen atom of DMSO as the stronger acceptor, and the N−H anti proton of the primary amide group of **1** as the weaker donor forms a hydrogen bond to the oxygen atom of the primary amide group of **1** as the weaker acceptor to give the catemer chain of the primary amide group, which leads to the 3-D hydrogen-bonded porous network of type A (Figure 12). In contrast, in the crystal structure of **1**·6*n*-PrOH, the N−H anti proton of the primary amide group of **1** as the weaker donor forms a hydrogen bond to the oxygen atom of *n*-PrOH as the weaker acceptor, and the N−H syn proton of the primary amide group of **1** as the stronger donor forms a hydrogen bond to the oxygen atom of the primary amide group of **1** as the stronger acceptor to give the cyclic dimer of the primary amide group, which leads to the 3-D hydrogen-bonded porous network of type B.

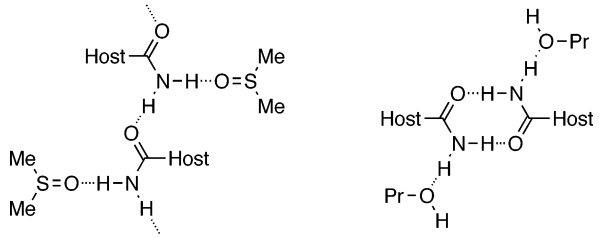


***Figure 12.*** Schematic representation for the correlation between hydrogen bond donor and acceptor among the primary amide group of **1**, DMSO, and *n*-PrOH.

The third factor is attributed to the polarity of the bulk crystallization solvents. The oxygen atom of $H_2O$ is the weakest hydrogen bond acceptor among the solvents used in the present work.[35] In fact, when **1** was crystallized from a 1:1 boiling mixture of $H_2O$ and *n*-PrOH, only single crystals of **1**·6*n*-PrOH were produced. On the other hand, $H_2O$ is the strongest hydrogen bond donor and the most polar solvent[35] in which hydrophobic and aromatic $\pi-\pi$ interactions act as the most effective attractive forces.[36] It might be possible that the $H_2O$ molecule could serve as a hydrogen bond acceptor or donor guest to fill a hydrogen-bonded porous network such as type B. This was not the case for the crystal formation of **1** under hydrothermal conditions. In the crystallization of **1** under hydrothermal conditions, the hydrophobic and aromatic $\pi-\pi$ interactions of **1** itself would be more favorable than the hydrogen bond of $H_2O$ with the amide group of **1**.[37] As a result, the nonporous 3-D hydrogen-bonded network chain of type C was formed in **1**·$H_2O$. The type C network could be likened to type B by changing the hydrogen-bonding motifs of the primary amide groups in part from cyclic dimers to catemer chains, by sharpening a puckering angle of **1** with respect to a plane containing a 2-D sheet ($\theta = 108°$ for **1**·$H_2O$ vs $\theta = 143.6°$ for **1**·6*n*-PrOH), and by an interdigitation of **1** into a network cavity to maximize the hydrophobic and aromatic $\pi-\pi$ interactions of **1** itself (Figure 7a,c vs Figure 9a,b,e).

Thus, a combination of the three factors discussed above plays an essential role in the solvent-induced topological isomerism of the 3-D hydrogen-bonded networks of the hexakis(primary amide) host **1**.

## Conclusion

Hexakis(4-carbamoylphenyl)benzene (**1**) as a new host molecule directed toward microporous organic solids has been

(33) Abraham, M. H.; Platts, J. A. *J. Org. Chem.* **2001**, *66*, 3484−3491 and references therein.
(34) The $\beta_2^H$ and $\alpha_2^H$ values, indicating the hydrogen bond basicity and acidity of *n*-PrOH, are 0.45 and 0.32, respectively.[33]
(35) Kamlet, M. J.; Abboud, J.-L. M.; Abraham, M. H.; Taft, R. W. *J. Org. Chem.* **1983**, *48*, 2877−2887.
(36) (a) Jorgensen, W. L.; Severance, D. L. *J. Am. Chem. Soc.* **1990**, *112*, 4768−4774. (b) Fujita, M.; Fujita, N.; Ogura, K.; Yamaguchi, K. *Nature* **1999**, *400*, 52−55.
(37) A reviewer suggested that high pressure under hydrothermal conditions would also play an important role in the network formation of type C.

synthesized, and characteristics of the network morphology have been examined. We have demonstrated the three types of 3-D hydrogen-bonded networks of **1** without self-interpenetration, in which solvent-induced topological isomerism of the 3-D hydrogen-bonded networks has been found: a porous network of type A in **1**·12DMSO, a porous network of type B in **1**·6*n*-PrOH, and a nonporous network chain of type C in **1**·$H_2O$ are composed of only catemer chains, only cyclic dimers, and a mixed type of helical catemer chains/cyclic dimer/catemer, respectively, as hydrogen-bonding motifs of primary amide groups. This solvent-induced topological isomerism of the 3-D hydrogen-bonded networks would be attributed to (i) the radially functionalized hexagonal structure of **1**, which provides a porous network to include guest solvents without self-interpenetration, (ii) the correlation between the hydrogen bond donor ability of the syn and anti protons of the primary amide group in host **1** and the hydrogen bond acceptor ability of the oxygen atoms of **1** and guest solvents, and (iii) the solvent polarity leading to hydrophobic and aromatic $\pi-\pi$ interactions. The present results suggest that the network morphology of a 3-D hydrogen-bonded porous network in an organic host lattice without self-interpenetration would be affected by the properties of the crystallization solvents.

## Experimental Section

**General Considerations.** 1,2-Dichloroethane was distilled from $CaH_2$ under $N_2$. The other solvents and all reagents were commercially available and used without any purification. $^1$H and $^{13}$C NMR spectra were recorded at 270 and 67.8 MHz, respectively, on a JEOL JNM-EX270 spectrometer. IR spectrum was recorded on a Jasco FT/IR-460Plus spectrometer. Thermal gravimetry (TG) was performed on a Seiko EXSTAR6000 system: using ~5 mg and heating from 35 to 450 °C at a heating rate of 5 °C min$^{-1}$.

**Hexakis(4-carbamoylphenyl)benzene (1).** To a heterogeneous mixture of hexakis(4-carboxyphenyl)benzene (**2**;[14b] 300 mg, 0.376 mmol) and benzyltriethylammonium chloride (86.7 mg, 0.467 mmol) in dry 1,2-dichloroethane (30 mL) under an argon atmosphere was added thionyl chloride (1.2 mL, 16.5 mmol). The mixture was stirred at 85 °C for 24 h and then was evaporated in vacuo under reduced pressure at room temperature. To the resulting solid was added a solution of 4-(dimethylamino)pyridine (27.9 mg, 0.228 mmol) in dry 1,2-dichloroethane (30 mL) under argon. Ammonia gas was slowly bubbled into the resulting solution at −40 °C for 45 min, and then the resulting mixture was warmed to room temperature overnight. The resulting precipitate was filtered, washed with $CH_2Cl_2$, water, MeOH, and ether, and dried to give 280 mg of **1** (94% yield) as a white solid: mp >450 °C; $^1$H NMR (270 MHz, DMSO-$d_6$) $\delta$ 6.96 (d, $J$ = 8.1 Hz, 12H), 7.20 (s, 6H), 7.39 (d, $J$ = 8.1 Hz, 12H), 7.73 (s, 6H); $^{13}$C NMR (67.8 MHz, DMSO-$d_6$, 80 °C) $\delta$ 126.0, 130.6, 131.2, 139.4, 142.1, 167.1; IR (KBr) 3349, 3187, 1661, 1611, 1557, 1406 cm$^{-1}$. Anal. Calcd for $C_{48}H_{36}N_6O_6$: C, 72.72; H, 4.58; N, 10.60. Found: C, 72.43; H, 4.86; N, 10.36. Anal. Calcd for $C_{48}H_{36}N_6O_6$·12DMSO: C, 49.97; H, 6.29; N, 4.86. Found: C, 49.66; H, 6.41; N, 4.87.

**X-ray Data Collection and Crystal Structure Determinations.** X-ray diffraction data were collected on a Bruker CCD/Smart 1000 diffractometer with graphite-monochromated Mo K$\alpha$ radiation. The structures were solved by direct methods (SHELXS-97 or SIR 92)[38,39] and refined with full-matrix least-squares procedures using the program teXsan.[40] All non-hydrogen atoms were refined with anisotropic displacement parameters. All hydrogen atoms were placed in idealized positions, and no further refinement was applied. The measurement conditions and structural details are listed in Table 1 (see also the Supporting Information).

**Acknowledgment.** We thank Dr. Ken Endo (Akita University) for the calculation of molecular volumes of **1** and benzamide. This work was supported in part by Grants-in-Aid from the Ministry of Education, Science, Sports, Culture, and Technology of Japan (Nos. 14045233 and 14340217) and Nissan Science Foundation.

**Supporting Information Available:** X-ray experimental details in the form of a crystallographic information file (CIF). This material is available free of charge via the Internet at http://pubs.acs.org.

JA0293103

(38) Sheldrick, G. M. SHELXS-97; University of Göttingen, Göttingen, Germany, 1997.
(39) Altomare, A.; Cascarano, M.; Giacovazzo, C.; Guagliardi, A. SIR92. *J. Appl. Crystallogr.* **1993**, *26*, 343.
(40) TeXsan for Windows, Crystal Structure Analysis Package; Molecular Structure Corp., The Woodlands, TX, 1997.